



**FLYGTEKNISKA
FÖRSÖKSANSTALTEN**

The Aeronautical Research
Institute of Sweden

Q8263

**ON THE VARIATION IN CRACK-OPENING
STRESSES AT DIFFERENT LOCATIONS IN
A THREE-DIMENSIONAL BODY**

by

R.G. Chermahini and A.F. Blom

RECEIVED BY.
ESA - IRS
DATE: 11 OCT. 1990
DCAF NO. 402655
PROCESSED BY
 NASA ST. FACILITY
 ESA - IRS AIAA

Stockholm 1990

(NASA-CR-187722) ON THE VARIATION IN
CRACK-OPENING STRESSES AT DIFFERENT
LOCATIONS IN A THREE-DIMENSIONAL BODY
(Aeronautical Research Inst. of Sweden)
29 p

N91-13768

Unclas
0320350

CSSL 20K G3/39



The Aeronautical Research
Institute of Sweden
Structures Department

ON THE VARIATION IN CRACK-OPENING STRESSES AT DIFFERENT LOCATIONS IN A
THREE-DIMENSIONAL BODY

by

R.G. Chermahini and A.F. Blom

ABSTRACT

Crack growth and closure behavior of thin and thick middle-crack tension specimens under constant amplitude loading were investigated using a three-dimensional elastic-plastic finite-element analysis of fatigue crack growth and closure. In the thin specimens the crack front closed first on the exterior (free) surface and closed last in the interior during the unloading portion of cyclic loading. The stabilized crack-opening stresses of thin ($t=4.78\text{mm}$) and thick ($t=12.7\text{mm}$) middle-crack tension specimens are determined at the interior and exterior regions under constant amplitude loading ($R=0.1$, $S_{\max}/\sigma_o=0.25$, σ_o is the effective yield stress). For the thin specimen the stabilized stress levels were found to be $0.34 S_{\max}$ and $0.56 S_{\max}$, whereas for the thick specimen the corresponding stress levels were $0.26 S_{\max}$ and $0.46 S_{\max}$, respectively.

A load-reduced displacement technique was used to determine crack-opening stresses at specified locations in the plate from the displacements calculated after the 7th cycle (using unloading and reloading portions of cyclic loading). All locations were on the plate exterior surface and were located near the crack tip (about 0.9 mm), behind the crack tip (about 4.30 mm) and at the centerline of the crack. With this technique the opening stresses at the specified points were found to be 0.52 , 0.42 and 0.39 times the maximum applied stress.

Sponsoring Agencies: The Defence Material Administration (FMV) and
NASA Langley Research Center

CONTENTS

	Page
NOMENCLATURE	5
1 INTRODUCTION	7
2 NUMERICAL ANALYSIS	8
3 SPECIMEN CONFIGURATION AND LOADING	10
4 RESULTS AND DISCUSSION	11
5 CONCLUSIONS	14
6 ACKNOWLEDGEMENTS	15
7 REFERENCES	15
FIGURES	17

NOMENCLATURE

b	half-width of specimen,	mm
c	half-length of crack,	mm
c_i	half-length of initial crack,	mm
d	smallest element size along crack plane,	mm
E	modulus of elasticity,	MPa
h	half-height of specimen,	mm
R	stress ratio (ratio of minimum to maximum applied stress)	
S	applied stress,	MPa
S_o	crack-opening stress,	MPa
S_{max}	maximum applied stress,	MPa
t	half-thickness of specimen,	mm
t_i	thickness of i^{th} layer,	mm
V	displacement in y-direction,	mm
σ_o	effective yield stress,	MPa

1 INTRODUCTION

The growth of a surface or through crack in a structural component is a three-dimensional process. Near regions where a crack intersects a free surface, the material is under plane-stress conditions. However, the crack front in the interior of the body may be under plane-strain conditions. Previous experiments and analyses have shown that the crack closure behavior is greatly affected by the state of stress. Closure under plane-stress conditions is much greater than that under plane-strain conditions.

During the past two decades many researchers have used Elber's crack-closure concept [1-3] to explain various experimentally observed fatigue crack growth phenomena and also for prediction of fatigue crack growth under various load histories. Several researchers [4-14] have analyzed the behavior of crack growth and closure of specimens under various load histories under both plane stress and plane strain conditions using two dimensional elastic-plastic finite-element analysis.

However, the crack closure behavior of finite-thickness plates under cyclic loading is not fully understood and two-dimensional finite-element techniques cannot be used for analyzing these specimens. In order to analyze crack growth and closure behavior of finite thickness plates, a three-dimensional elastic-plastic finite-element technique was developed [15]. The model was used to determine crack-opening and closure stresses of a middle-crack tension (MT) specimen both under constant and variable amplitude loading [16] and also to study the influence of specimen thickness on the computed crack opening stress levels [17].

The purpose of the present study is to investigate crack growth behavior of thin and thick MT- specimens under constant amplitude loading conditions. The stabilized crack opening stresses of interior and exterior regions and the closure and opening profiles of the crack-surface plane after the 10th cycle are presented for both thin and thick plates. The effect of thickness on crack opening stress levels, and plastic zones of interior and exterior regions is demonstrated for the thick specimen after 10 cyclic loadings.

To determine the crack-opening stresses at specified points on the thin plate exterior surface, a load-reduced displacement technique was used based on displacements calculated after the 7th cycle (using unloading and reloading portions of cyclic loading). This technique is similar to the compliance techniques used by most experimentalists to measure crack opening load levels. All analyses are performed under constant amplitude-loading ($R=0.1$) assuming elastic-perfectly plastic conditions.

2 NUMERICAL ANALYSIS

The three-dimensional elastic-plastic finite element procedure used to simulate crack extension and crack closure has been described in detail elsewhere [15]. Here, only a brief summary is given.

The middle-crack tension specimen (Fig.1) is modelled with linear eight-noded isoparametric solid elements (Fig.2). Due to symmetry conditions, only one-eighth of the specimen was analysed.

2.1 Elastic analysis

The small-strain theory, linear-elastic material properties and a 2x2x2 quadrature scheme were used to calculate the element stiffness matrix [18]. The equations of equilibrium were obtained from the principle of minimum total potential energy and are expressed as

$$[K_e] \{U\} = \{P\} \quad (1)$$

where matrices K_e , U and P represent total structural stiffness, nodal displacements, and applied loads, respectively. Equation (1) was solved using Cholesky's factorization technique. The stresses and strains were evaluated at the eight quadrature points in the element.

2.2 Elastic-plastic analysis

The elastic-plastic analysis was based on Zienkiewicz et al., initial stress method [19]. Yielding was evaluated at every quadrature point using the von Mises yield criterion. Stresses in excess of the yield stress (for an elastic perfectly plastic material) were redistributed

using Drucker's normality flow rule [20]. The analysis used small-strain and incremental plasticity theory. The complete algorithm is given in ref. [19]. The main advantage of this method is the repeated use of the factorized elastic stiffness matrix. The equations of equilibrium which govern the elastic-plastic deformation are

$$[K_e]\{U\}=\{P\}+\{Q\} \quad (2)$$

where Q is the plastic-load vector. The Q forces maintain the plastic strains in the elements. In the initial-stress method, the solution to an elastic-plastic problem is obtained by applying a series of small load increments to the structure until the desired applied load is reached. The load increment was chosen as 20% of the load required to yield the first element. At each load increment, eq.(2) was solved iteratively. The iteration process was repeated until the effective stress was within 2% of the yield stress in all yielded elements. Usually 5 to 15 iterations were required for convergence.

2.3 Crack extension and closure analysis

Fatigue-crack growth simulation involves opening and closing of the crack surfaces, which leads to a variable boundary-value problem. In ref. [4], an algorithm is given to modify the factorized stiffness matrix to change the appropriate boundary conditions. The technique involves introducing a very stiff spring to restrain a boundary displacement or removing the spring to free a displacement restraint (to open the crack). The "rigid" spring stiffness (10^7 times the modulus of elasticity) was added to the diagonal coefficient in the conventional elastic stiffness matrix. To extend the crack, the stiffness of the springs at the crack front was set equal to zero in the modified stiffness matrix K_e and the forces F that were carried by the springs were then applied to the crack-front nodes. The equilibrium equations are

$$[K_e]\{U\}=\{P\}+\{Q\}+\{F\}. \quad (3)$$

The nodal forces F , used only during crack extension, were arbitrarily chosen to be released in five equal load steps to advance the crack front. To insure that the stress and total strain increments in the adjacent elements satisfied the appropriate yield conditions and flow rule, the iterative analysis [19] was repeated and the forces previously carried by the broken springs were released and redistributed.

During cyclic loading, the nodal displacement along the crack plane were monitored to determine whether the crack surfaces at any node were to open (positive displacement) or close (negative displacement). If the crack surfaces should open, the stiffness of the boundary spring would be set equal to zero and the stiffness matrix would be updated. If the crack surfaces should close, the spring stiffness would be set to an extremely large value and the stiffness matrix would again be updated. No attempt was made in any of the analyses to include a failure criterion for crack extension. The crack was extended one element size (0.03mm) per cycle when the maximum applied stress was reached.

3 SPECIMEN CONFIGURATION AND LOADING

A middle-crack tension specimen (Fig. 1) was studied under constant amplitude loading ($R = 0.1$, $S_{\max}/\sigma_0 = 0.25$) in all the analyses. The material was assumed to be elastic-perfectly plastic. The dimensions of the specimen were $b = 38.1$ mm, $h = 2b$ and $t = 4.78$ mm and 12.7 mm, respectively. The crack was extended by one element size (0.03 mm) at the maximum applied stress of each load cycle. The initial crack length c_1 was 18.6 mm. The modulus of elasticity E was 70 000 MPa, Poisson's ratio was 0.3, and the effective yield stress σ_0 was 345 MPa. The finite-element idealization of the model is shown in Fig. 2. Because the specimen configuration and loading were symmetric, only one-eighth of the plate was modeled. A four-layer model was used in the present analysis. The layer thicknesses (t_i) were chosen as $0.5t$, $0.25t$, $0.15t$, and $0.1t$ where the smallest layer was located on the exterior (free) surface of the specimen ($z = t$). The mesh had 3804 elements and 5145 nodes with 15435 degrees-of-freedom. For purposes of discussion, the $Z=0$ plane is referred to as the "interior" plane and the $Z=t$ plane as the "exterior" plane. Figure 2 also shows elements on the "interior layer" and "exterior layer".

4 RESULTS AND DISCUSSION

First, the analysis was applied to the thinner specimen ($t=4.78\text{mm}$). The stabilized opening stresses for interior and exterior regions after the 10th cyclic loading, already reported in Ref. [16], were found to be 0.34 and 0.56 times the maximum applied stress (S_{max}), respectively, as shown in Fig.3. Next, the same finite-element mesh was used and the thickness of the layers was increased. The specimen thickness was 12.7 mm and the model was exercised under the same type of loading which was used for the thinner plate. The stabilized crack-opening stresses of interior and exterior regions after 33 cycles were found to be 0.26 and 0.46 times the maximum applied stress (S_{max}), respectively, as shown in Fig.4.

The drop in opening loads can be explained as follows. The constraint effect at the interior region ($z=0$ plane), causes a variation in displacements through the specimen thickness which gives different opening loads for interior and exterior regions, respectively.

The interior region ($z=0$ plane) is considered to be under plane strain conditions, whereas the exterior region ($z=t$ plane) is approximately under plane stress conditions. The crack-opening stress level of the interior region first reached a maximum peak ($S_o/S_{\text{max}}=0.34$) and then upon further crack-extension dropped to a ratio of 0.28. A similar trend in crack opening stress is reported by Fleck and Newman [14] under plane-strain conditions. The exterior region crack-opening stress level experiences a similar behavior and dropped to a ratio of 0.52. The constraint effect which gives different deformations on the interior and exterior regions of a three-dimensional model, causes a variation in opening stresses through the specimen thickness. The crack-opening stresses of thin and thick specimens through specimen thickness are shown in Fig.5. The thinner plate crack-opening stress level of the interior region is less than that of thick plate, whereas the crack-opening stress level of the thin plate for the exterior region is higher than that for the thick plate.

The closure and opening profiles of the crack-surface plane for the 10th load cycle of the thinner specimen, already reported in Reference [16], are shown in Fig. 6. The interior region is fully open at the stress level of $0.36 S_{\max}$. At a stress level of $0.56 S_{\max}$, the surface nodes behind the crack-tip node are still closed. As soon as the applied stress reaches beyond $0.56 S_{\max}$, the entire crack-plane is fully open.

The closure and opening profiles of the crack-surface plane for the 10th load cycle of the thicker specimen are shown in Fig. 7. At the stress level of $0.34 S_{\max}$, the interior is fully open while the surface nodes behind the crack-tip node are still closed. As the applied stress reaches beyond $0.34 S_{\max}$, the entire crack surface plane is fully open. Clearly, the thicker specimen has a smaller surface layer influenced by the state of "plane stress" at the free boundary, due to more plastic constraint, and consequently the overall crack closure behaviour is more dominated by the interior plane strain region. In this analysis, the thick specimen had the same thickness ratio (thickness layer over plate thickness) as the thin plate. To obtain a better result, the thick plate with several layers should be used in the analysis.

The effect of constraint can also be visualized by comparing the size of the plastic zones resulting from different deformations through the specimen thickness after the 10th cyclic crack extension for the interior and exterior regions of the thick specimen as shown in figs.8 and 9, respectively.

4.1 Load-reduced-displacement compliance technique

The load-reduced-displacement technique is frequently used by experimentalists to obtain the crack-opening stress from displacements measured at various locations along the crack plane. Here, the load-reduced-displacement technique was used to derive crack-opening stress levels from displacements at specified locations A_1 , A_2 and A_3 along the crack plane on the outer surface for the thin specimen ($t=4.78$ mm), (see Fig. 10). The A_1 location was first chosen by Elber [3] to make his experimental measurements. Location A_2 is 4.30 mm behind the crack front. The A_3 location is at the center of the specimen which is commonly chosen for experimental measurement of crack-opening stress levels.

The applied stress is plotted against the crack-opening displacement for the specified points A_1 , A_2 and A_3 as shown in Fig. 10. These curves are constructed using the displacements calculated for 65 load increments. Points A_2 and A_3 , which lie on the crack surface, give larger crack-opening displacements than point A_1 . However, the displacements at point A_1 should be more sensitive to the closure behavior on the outer region of the model. Figs. 11 to 13 show the load-reduced displacement plots for points A_1 , A_2 and A_3 , respectively. These load-reduced displacement plots were obtained using the following steps.

A straight line is fitted through unloading points of the 7th cyclic loading. Knowing the equation of this line, an expression for the displacement quantities is obtained. For each load increment, the corresponding displacement quantity is then found from the equation of the straight line. The difference between the finite element calculation and the straight-line displacement is called the reduced displacement which is due to the effects of plasticity.

The applied stress and reduced displacement quantities were found using the unloading and reloading portions of the cyclic load history. For unloading and the range of applied stress between 86.2 MPa and 68.95 MPa, the reduced displacement values are zero. Between 68.95 MPa and 41.37 MPa stress range, the reversed plasticity at the crack front causes the reduced displacement values to decrease. Below 41.37 MPa, reversed plasticity and crack closure causes erratic behaviour of the reduced displacement plot. Crack closure tends to increase the reduced displacement value (opposite to that caused by reverse plasticity). At the minimum applied stress, $S_{\min} = 8.62$ MPa, the maximum reduced displacement value was obtained. For the reloading portion of the load history, the curve goes to the left because the crack-surfaces are opening behind the crack front. For the point at which $\partial S / \partial \Delta V = \infty$, the crack-opening stress was obtained. The crack-opening stress for point A_1 was found to be 45 MPa. Upon further reloading, the curve moved to the right and came back to its starting point.

A similar trend was found for points A_2 and A_3 . The crack-opening stresses for points A_2 and A_3 , using the load-reduced displacement plot, were found to be 36 and 34 MPa in Figs 12 and 13, respectively.

The normalized crack-opening stress, as a function of normalized distance from the center of the crack for points A_1 , A_2 and A_3 is shown in Fig. 14. Based on these results, it can be seen that point A_1 has a reduced displacement crack-opening stress close to the outer region reduced displacement crack-opening stress. On the other hand, point A_3 has a reduced displacement crack-opening stress level closer to the inner region value. The reduced displacement crack-opening stress for point A_2 is located between the crack-opening stresses of points A_1 and A_3 .

5 CONCLUSIONS

The three-dimensional model was applied to middle crack tension specimens with two different thicknesses to investigate crack growth and closure behavior under constant amplitude loading. A load-reduced displacement technique was used to calculate the crack opening stresses at specified locations on the crack surface plane. Results from the analysis support the following conclusions:

- i) The crack opening stress level in the interior region is lower than that for the exterior region of the three-dimensional body which is due to the constraint effect. The effect of constraint on thickness gives a lower stabilized crack-opening stress level of $0.26 S_{\max}$ and $0.46 S_{\max}$ for the interior and exterior regions of the thick specimen than for the thin plate, where the same values became $0.28 S_{\max}$ and $0.52 S_{\max}$, respectively.
- ii) The crack-opening stresses at three specified locations on the crack-surface plane of the thin specimen ($t = 4.78$ mm) were calculated using a load-reduced-displacement technique. The normalized crack-opening stress, as a function of normalized distance from the center of the crack for points A_1 , A_2 and A_3 is shown in Fig. 14.

- iii) Closure values determined by the load-reduced-displacement technique (similar to experimental studies) approach those derived from the point of contact at the first crack tip node in the finite element solution. However, due to the smaller sensitivity of the load-reduced-displacement technique those values are dependent on location on the specimen surface. Close to the crack tip the value approaches the "plane stress" value, while far away from the crack tip a value close to the inner region "plane strain" result is obtained.

6 ACKNOWLEDGEMENTS

This work was supported by the NASA Langley Research Center through Grant No. NAG-1-529, and by the Defence Material Administration through TFFP 87/88:HU-2864. The authors are grateful to Dr. J.C. Newman, Jr. for helpful discussions during the course of this investigation.

7 REFERENCES

- [1] Elber, W., "Fatigue Crack Propagation", Ph. D. Thesis, University of New South Wales, Australia, 1968.
- [2] Elber, W., "Fatigue Crack Closure Under Cyclic Tension", Engineering Fracture Mechanics. Vol. 2, No. 1, July 1970, pp. 37-45.
- [3] Elber, W., "The Significance of Fatigue Crack Closure", ASTM STP-486, American Society for Testing and Materials, 1971, pp. 230-242.
- [4] Newman, J.C. Jr., "Finite-Element Analysis of Fatigue Crack Propagation - Including the Effects of Crack Closure". Ph. D. Thesis, VPI & SU, Blacksburg, VA, May 1974.
- [5] Newman, J.C. Jr., "A Finite-Element Analysis of Fatigue Crack Closure", Mechanics of Crack Growth, ASTM STP-490, American Society for Testing and Materials, 1976, pp. 281-301.
- [6] Newman, J.C. Jr. and Armen, Harry, Jr., "Elastic-Plastic Analysis of a Propagating Crack Under Cyclic Loading", AIAA Journal, Vol. 13, No. 8, August 1975, pp. 1017-1023.
- [7] Ohji, K., Ogura, K. and Ohkubo, Y., "Cyclic Analysis of a Propagating Crack and Its Correlation with Fatigue Crack Growth", Engineering Fracture Mechanics J., Vol. 7, 1975, pp. 457-464.

- [8] Nakagaki, M. and Atluri, S.N., "Elastic-Plastic Analysis of Fatigue Crack Closure in Modes I and II", *AIAA Journal*, Vol. 18, 1980, pp. 1110-1117.
- [9] Kobayashi, H. and Nakamura, H., "Investigation of Fatigue Crack Closure (Analysis of Plasticity Induced Crack Closure)", *Current Research on Fatigue Cracks*, The Society of Materials Science (Japan)., 1985, pp. 201-215.
- [10] Ogura, K., Ohji, K. and Honda, K. "Influence of Mechanical Factors on the Fatigue Crack Closure", *Fracture 1977*, Vol. 2, ICF4, Waterloo, Canada, June 19-24, 1977, pp. 1035-1047.
- [11] Liu, H.W., Yang, C.Y. and Kuo, A.S., "Cyclic Crack Growth Analyses and Modelling of Crack Tip Deformation", *Fracture Mechanics*, edited by N. Perrone, H. Liebowitz, D. Mulville and W. Pilkey, University Press of Virginia, Charlottesville, Virginia, 1978, pp. 629-647.
- [12] Blom, A.F. and Holm D.K., "An Experimental and Numerical Study of Crack Closure", *Engineering Fracture Mechanics J.*, Vol. 22, No. 6, pp. 997-1011, 1985.
- [13] Lalor, P.L. and Sehitoglu, H., "Fatigue Crack Closure Outside Small Scale Yielding Regime", *ASTM STP 982*, 1988.
- [14] Fleck, N.A. and Newman, Jr. J.C., "Analysis of Crack closure Under Plane Strain Conditions", *ASTM STP 982*, 1988.
- [15] Chermahini, R.G., "Three-Dimensional Elastic-Plastic Finite-Element Analysis of Fatigue Crack Growth and Closure", Ph. D, Thesis, Old Dominion University, Norfolk, VA., August 1986.
- [16] Chermahini, R.G., Shivakumar, K.N. and Newman, Jr. J.C., "Three-Dimensional Finite-Element Simulation of Fatigue-Crack Growth and Closure", *ASTM STP 982*, 1988
- [17] Chermahini, R.G., Shivakumar, K.N., Newman, Jr., J.C. and Blom, A.F., "Three-Dimensional Aspects of Plasticity - Induced Fatigue Crack Closure", *Engng Fracture Mech*, 34, 393-401 (1989).
- [18] Zienkiewicz, O.C., "The Finite Element Method", third edn. McGraw-Hill, London, U.K. (1977)
- [19] Zienkiewicz, O.C., Valliappan S. and King. I.P., "Elasto-plastic solutions of engineering problems: Initial stress, finite element approach". *Int. J. numer. Meth. Engng* 1, 75-100 (1969)
- [20] Drucker, D.C., "A more fundamental approach to plastic stress-strain solutions". *Proc. 1st U.S. Nat. Cong.appl.Mech* 487-491 (1951).

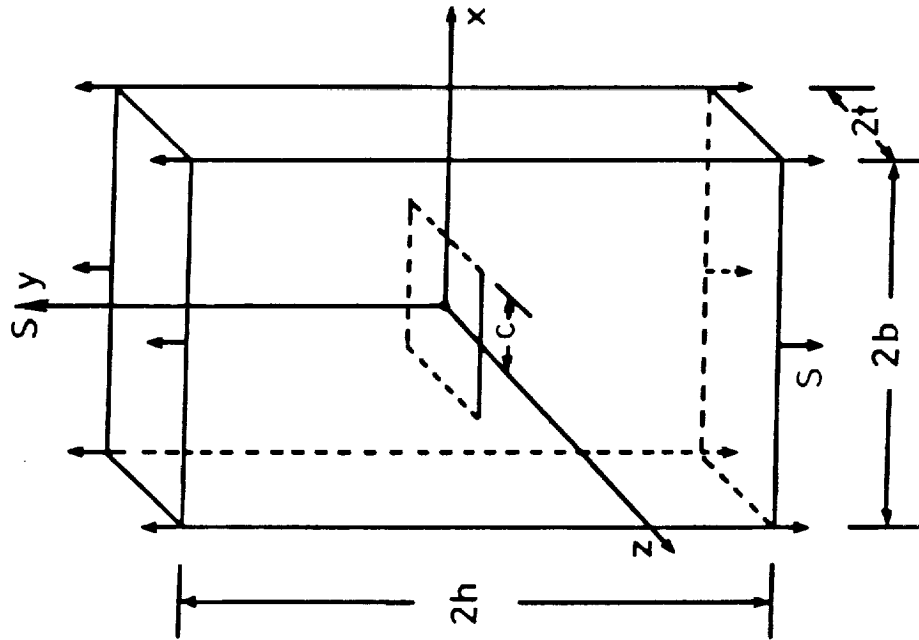


Fig. 1 Middle-crack tension specimen subjected to uniform stress

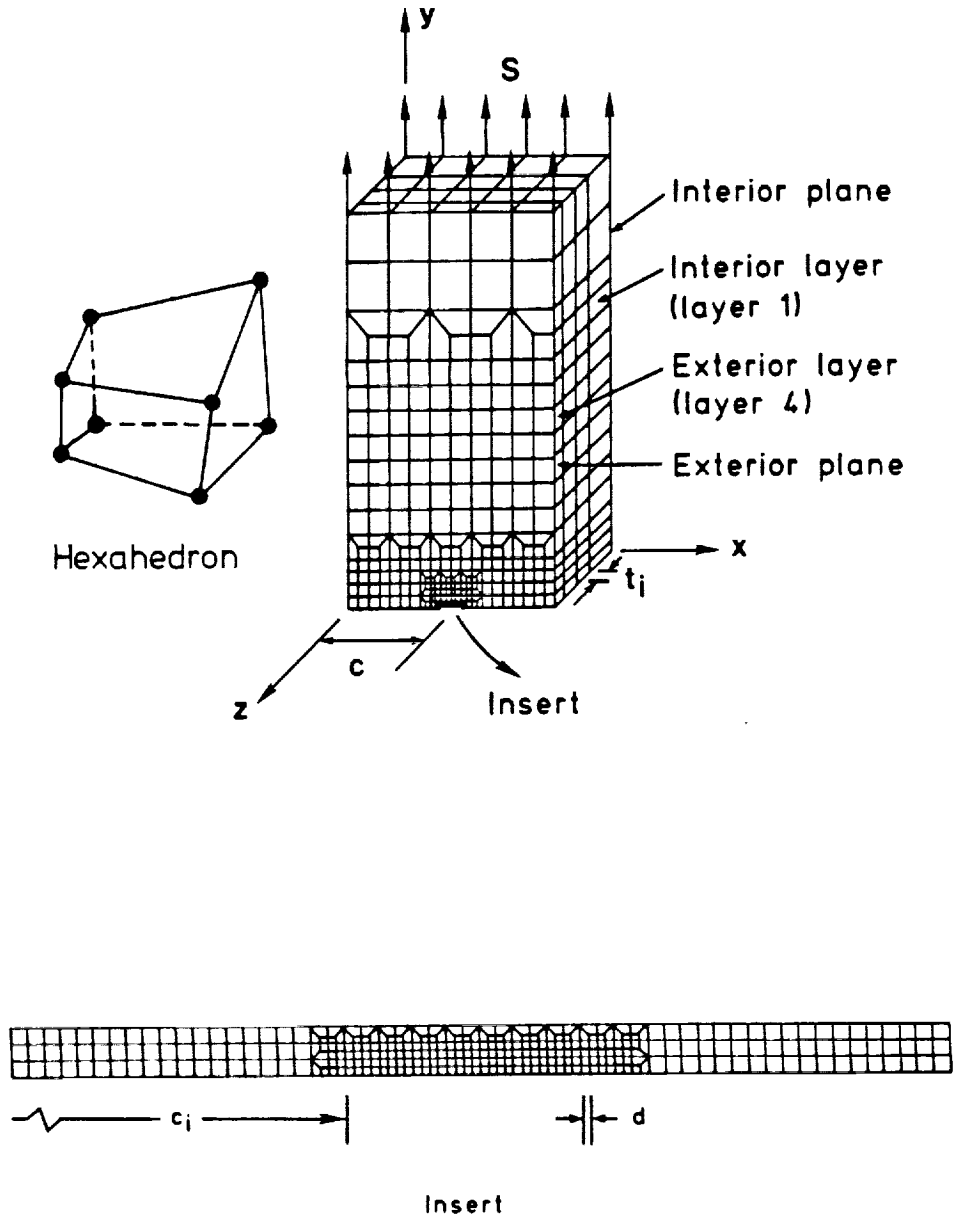


Fig.2 Finite-element idealization of middle-crack tension specimen

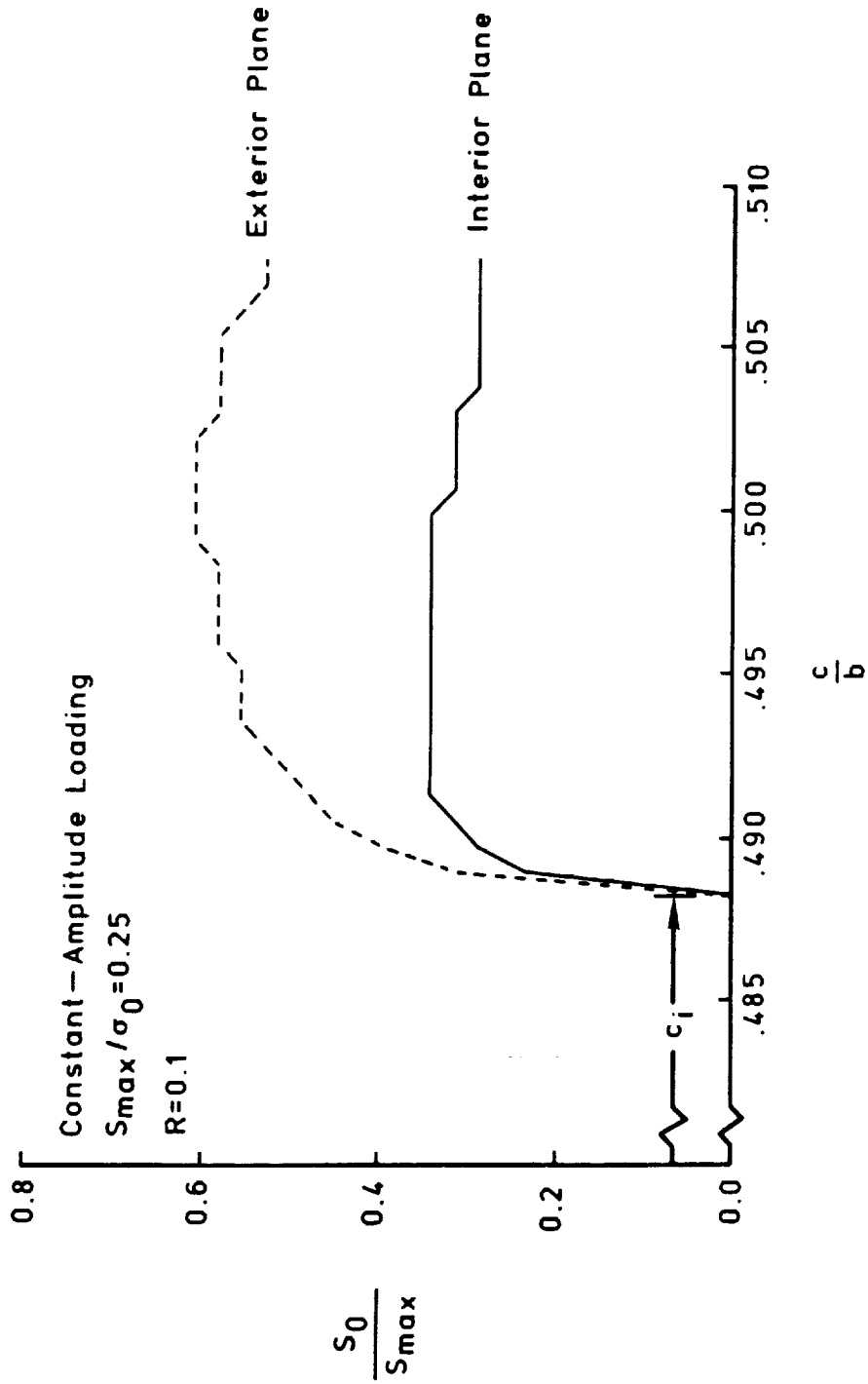


Fig. 3 Normalized crack-opening stresses on interior and exterior planes under constant-amplitude loading ($t=4.78$ mm)

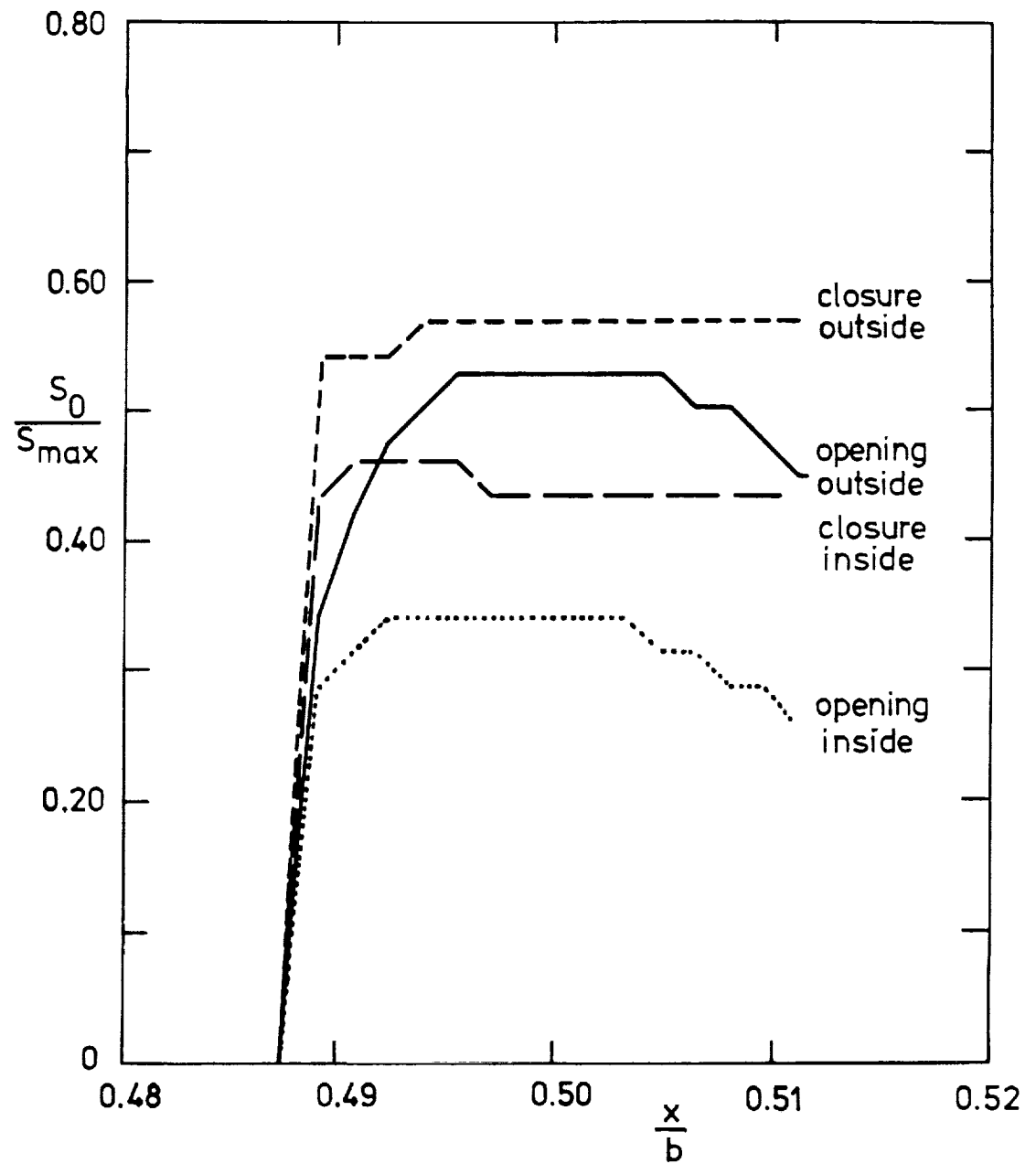


Fig. 4 Normalized crack-opening and closure stresses on interior and exterior planes under constant amplitude loading ($t = 12.7$ mm)

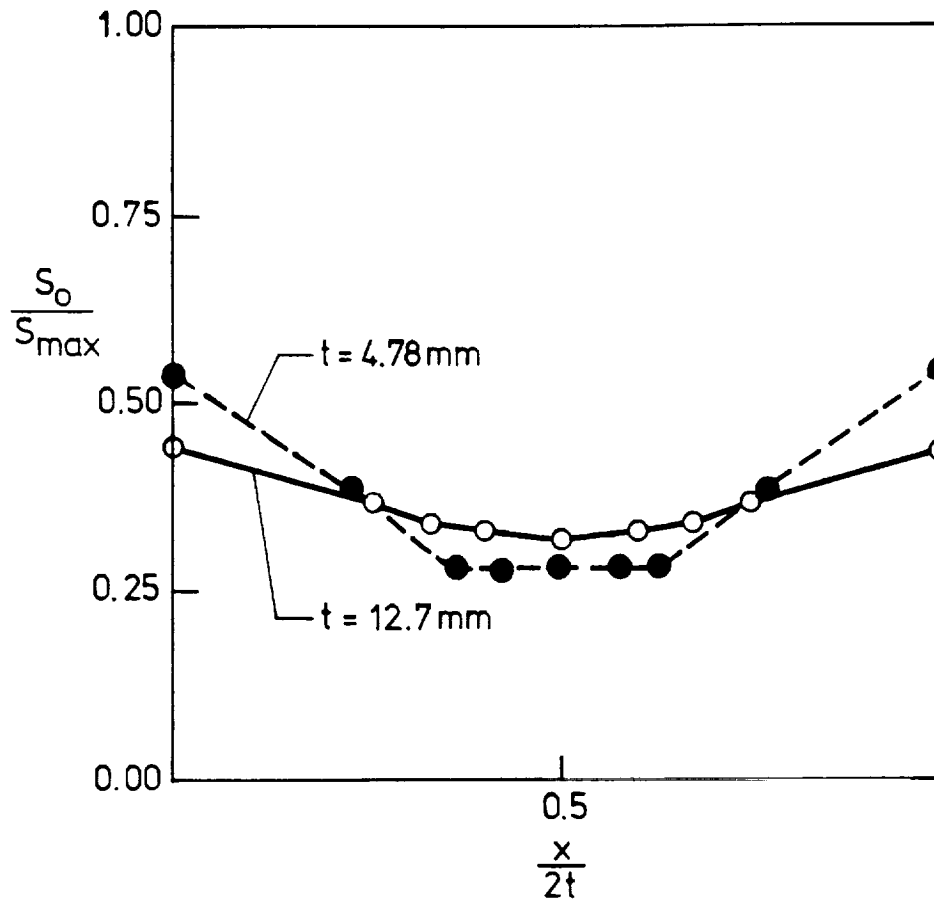


Fig. 5 Normalized crack-opening stress variation through the specimen thickness

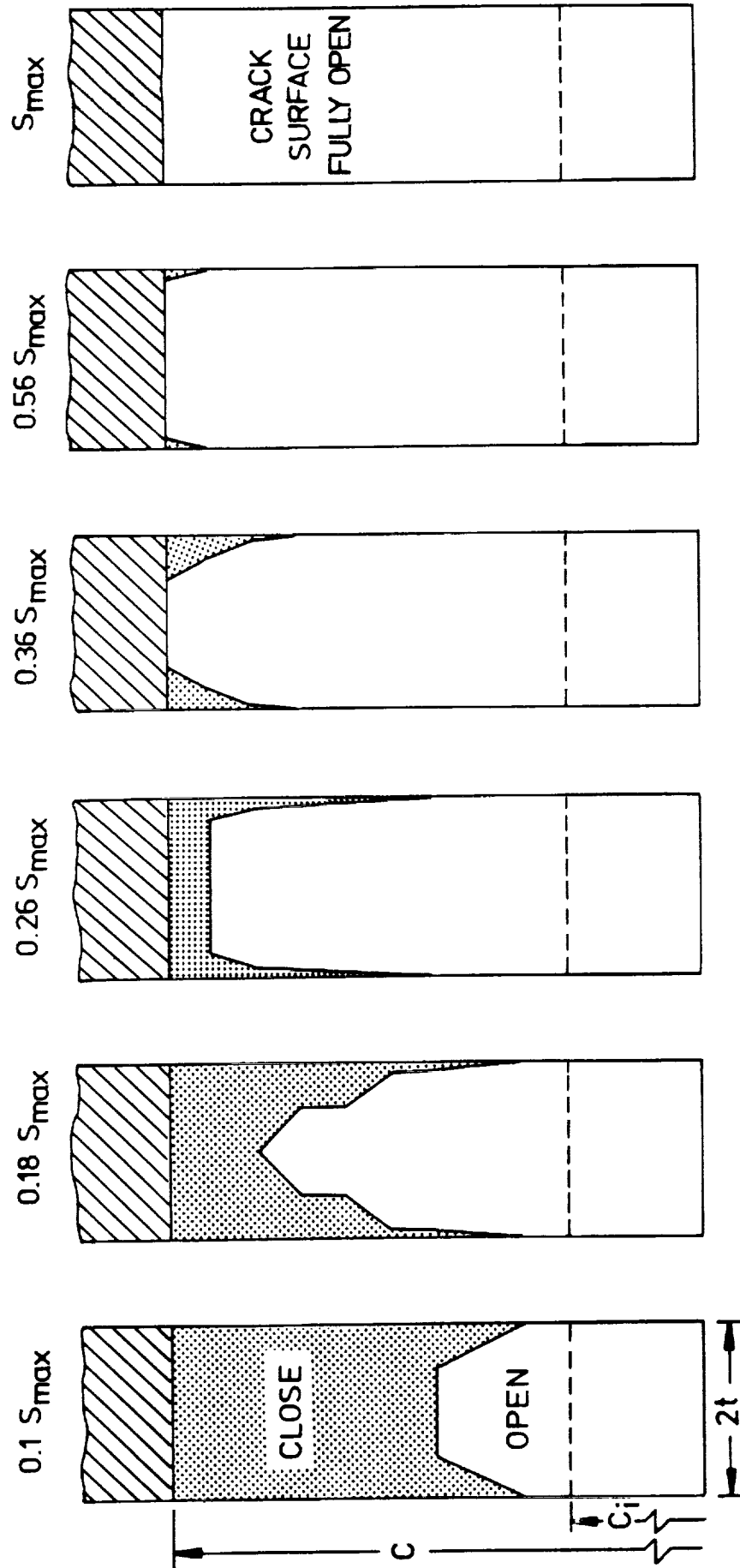


Fig. 6 Closure and opening profiles on the crack surface plane under constant-amplitude crack extension with $S_{max} = 0.25\sigma_0$ and $R = 0.1$ ($t=4.78$ mm)

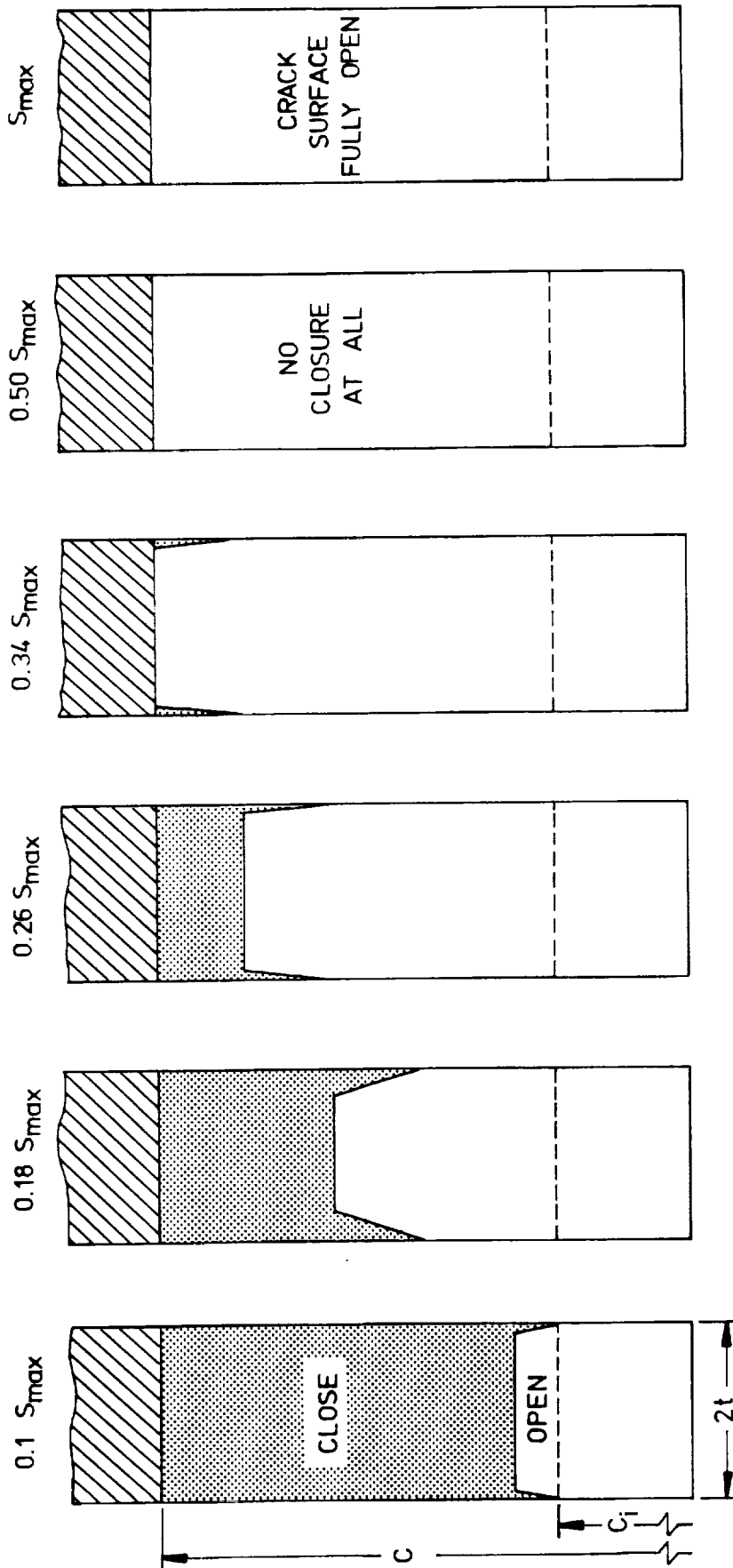


Fig. 7 Closure and opening profiles on the crack surface plane under constant amplitude crack extension with $S_{max} = 0.25 \sigma_o$ and $R = 0.1$ ($t=12.7$ mm)

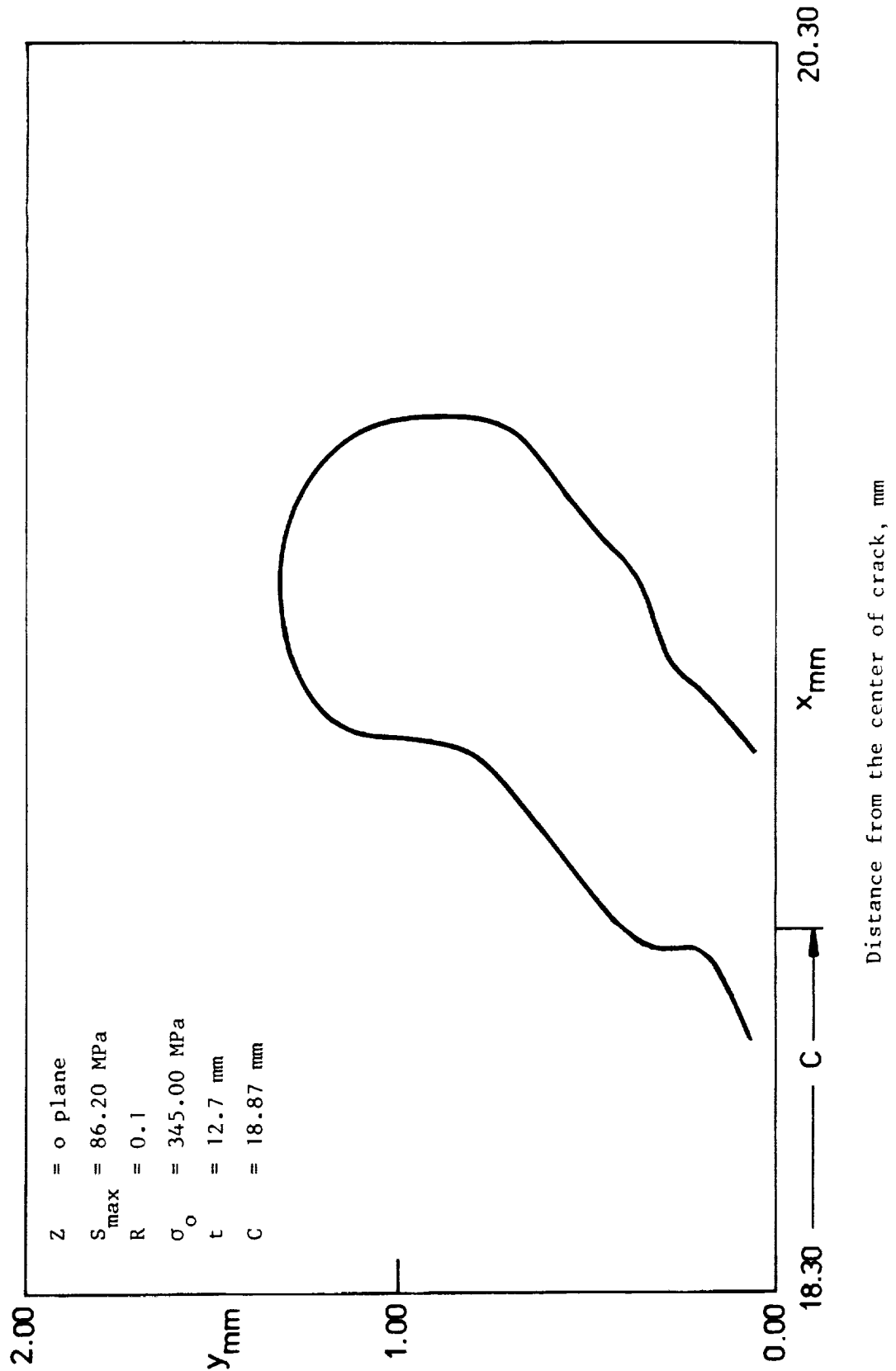


Fig. 8 The plastic zone size at the interior region after 10 cyclic crack extensions at the maximum applied stress

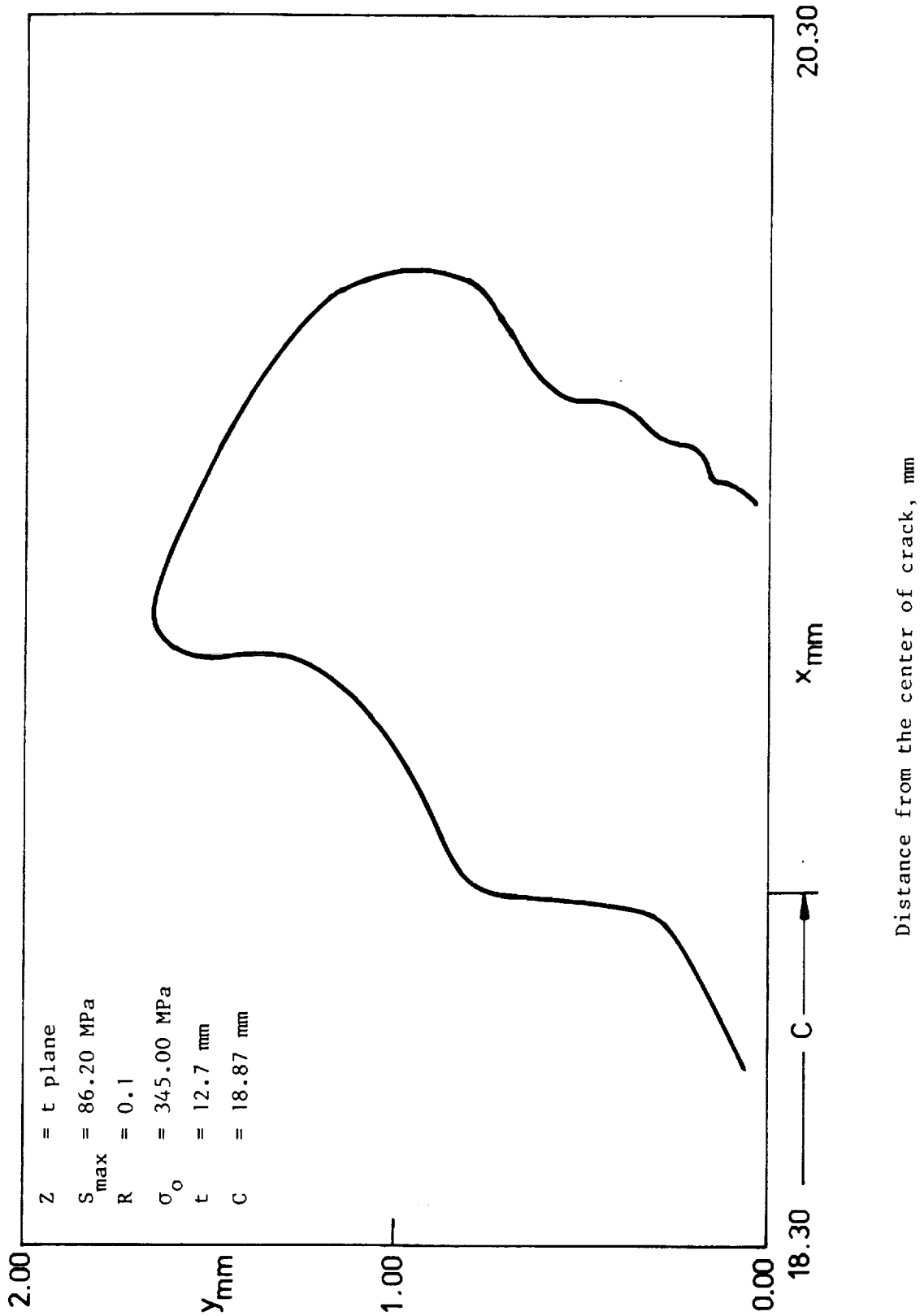


Fig. 9 The plastic zone size at the exterior region after 10 cyclic crack extensions at the maximum applied stress

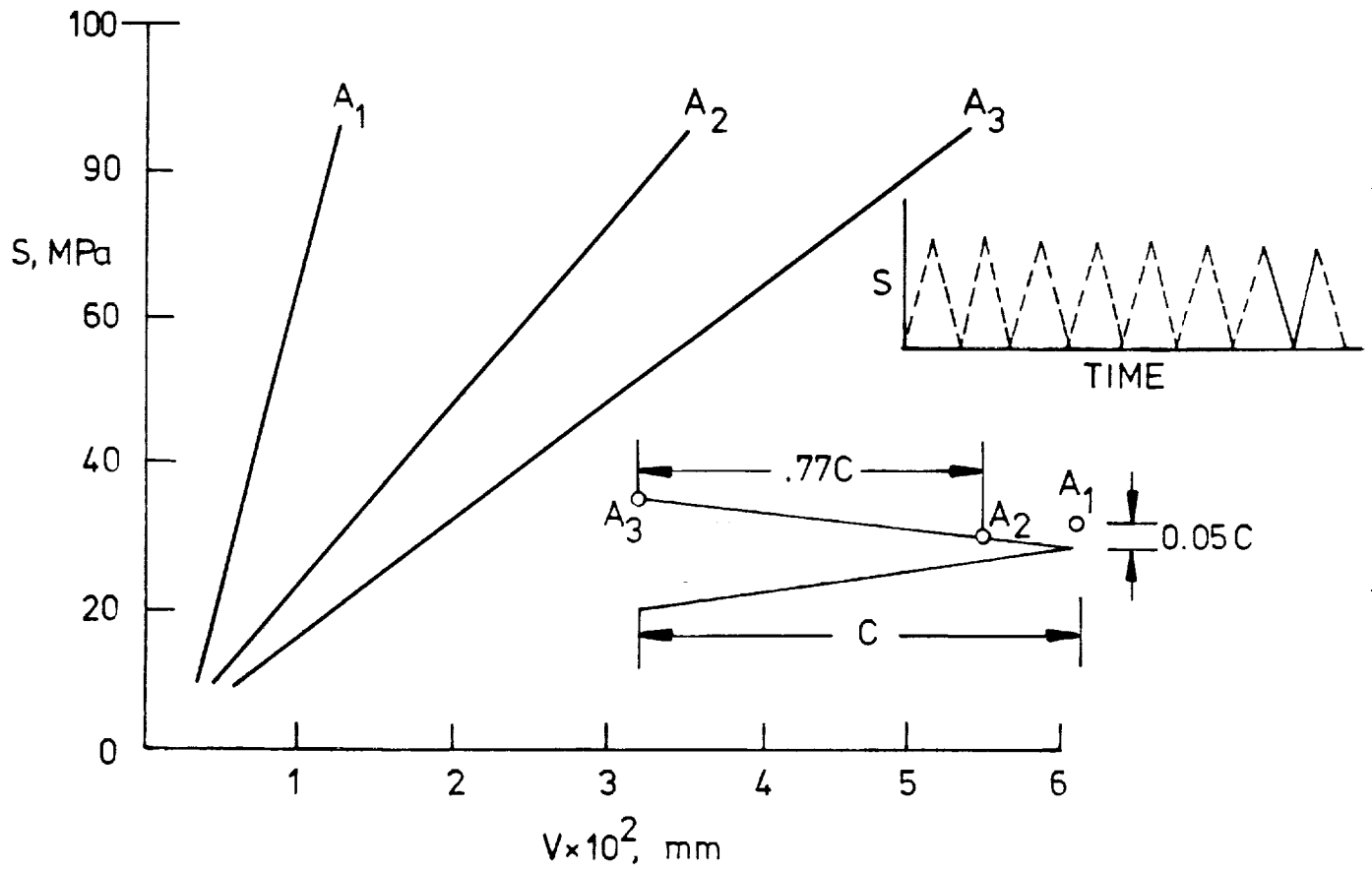


Fig. 10 Applied stress against crack opening displacement for specified points along crack plane

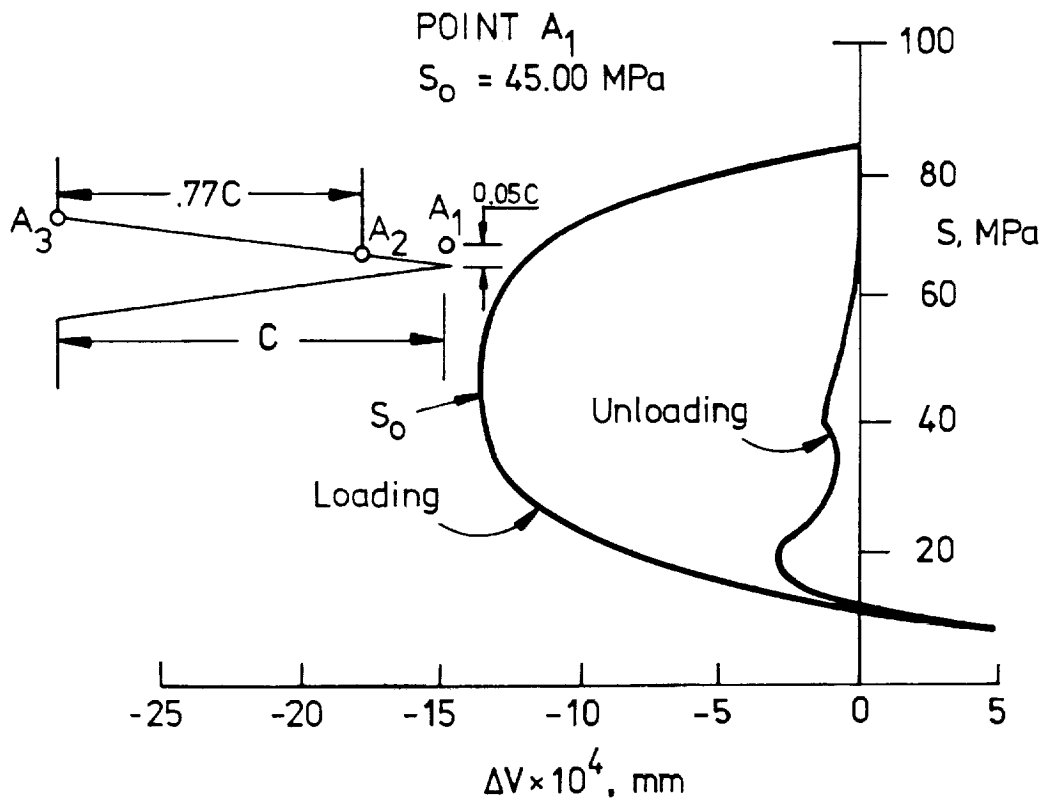


Fig. 11 Determination of crack-opening stress using a load-reduced-displacement technique for point A₁ (t=4.78 mm)

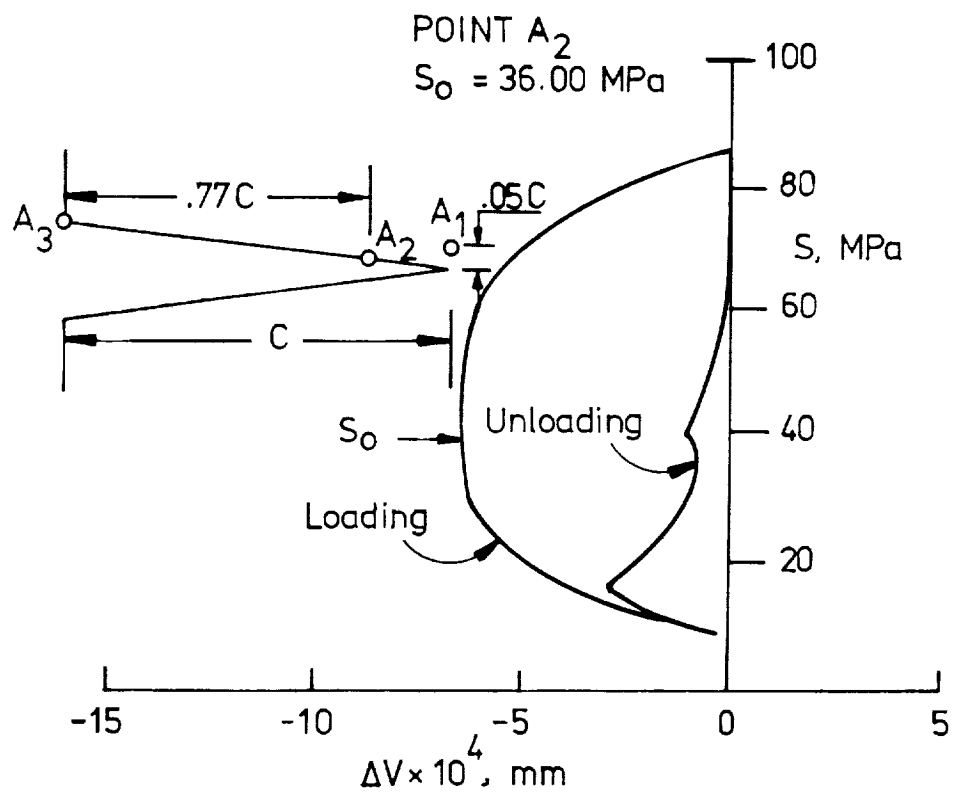


Fig. 12 Determination of crack-opening stress using a load-reduced-displacement technique for point A₂ (t=4.78 mm)

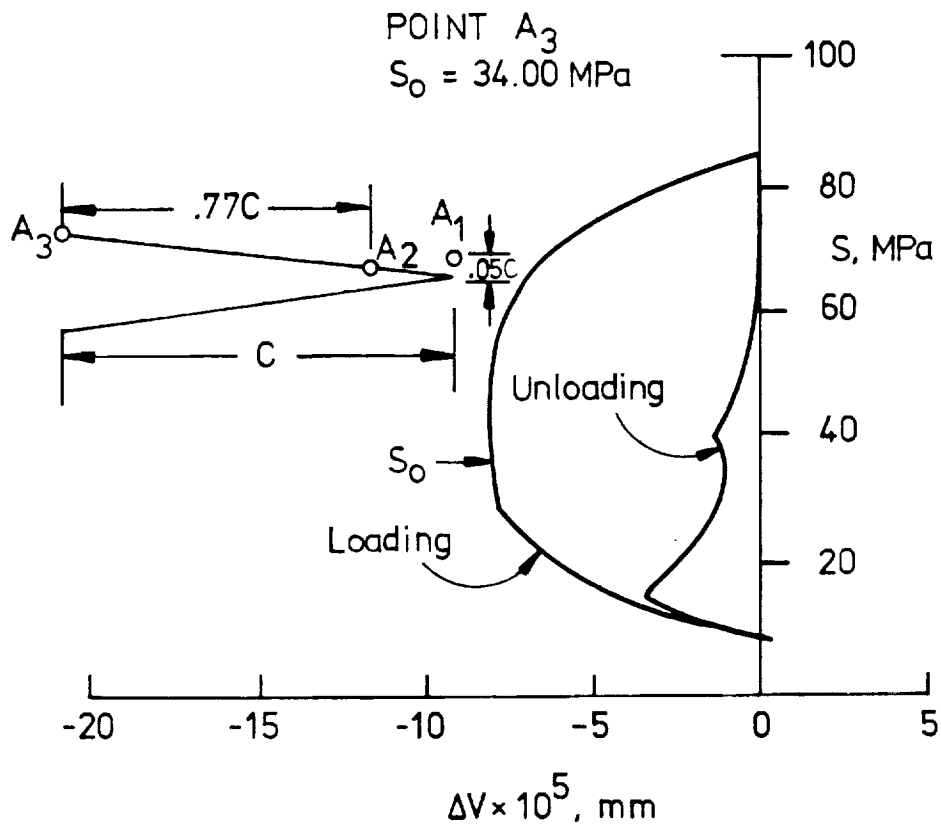


Fig. 13 Determination of crack-opening stress using a load-reduced-displacement technique for point A₃ (t=4.78 mm)

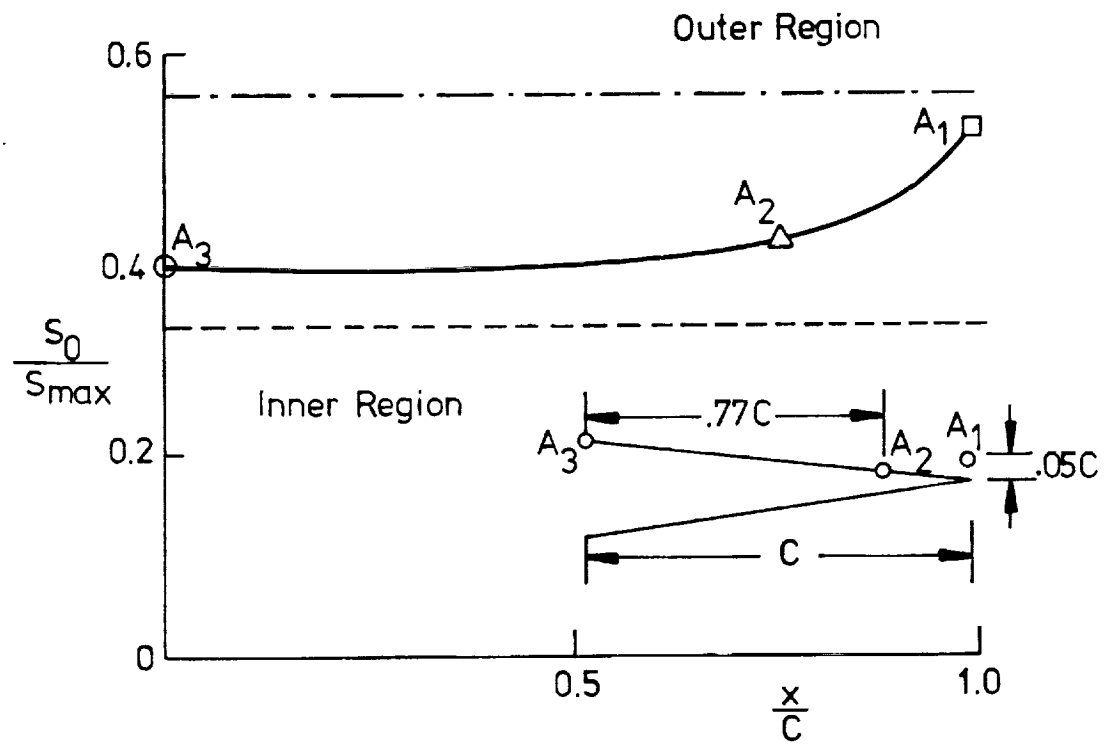
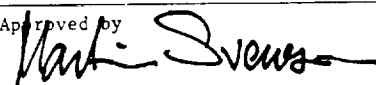


Fig. 14 Variation of crack opening stress for specified locations along the crack plane ($t=4.78$ mm)

Issuing organisation FLYGTEKNISKA FÖRSÖKSANSTALTEN The Aeronautical Research Institute of Sweden Structures Department Box 11021 S-161 11 BROMMA, Sweden		Document No. FFA TN 1988-21	
		Date September 1990	Security
		Reg. No. 683/90	Copy No. 36
Sponsoring agency The Defence Material Administration (FMV)		Project No. HU-2864 HU-2944	Order/contract TFFP 87/88 Test programme
Fdok			
Title ON THE VARIATION IN CRACK-OPENING STRESSES AT DIFFERENT LOCATIONS IN A THREE-DIMENSIONAL BODY			
Author(s) R.G. Chermahini and A.F. Blom		Work performed by	
Checked by		Approved by  Martin Svenson Head, Structures Department	
Abstracts <p>Crack growth and closure behavior of thin and thick middle-crack tension specimens under constant amplitude loading were investigated using a three-dimensional elastic-plastic finite-element analysis of fatigue crack growth and closure. In the thin specimens the crack front closed first on the exterior (free) surface and closed last in the interior during the unloading portion of cyclic loading. The stabilized crack-opening stresses of thin ($t=4.78\text{mm}$) and thick ($t=12.7\text{mm}$) middle-crack tension specimens are determined at the interior and exterior regions under constant amplitude loading ($R=0.1$, $S_{\max}/\sigma_0=0.25$, σ_0 is the effective yield stress). For the thin specimen the stabilized stress levels were found to be $0.34 S_{\max}$ and $0.56 S_{\max}$, whereas for the thick specimen the corresponding stress levels were $0.26 S_{\max}$ and $0.46 S_{\max}$, respectively.</p> <p>A load-reduced displacement technique was used to determine crack-opening stresses at specified locations in the plate from the displacements calculated after the 7th cycle (using unloading and reloading portions of cyclic loading). All locations were on the plate exterior surface and were located near the crack tip (about 0.9 mm), behind the crack tip (about 4.30 mm) and at the centerline of the crack. With this technique the opening stresses at the specified points were found to be 0.52, 0.42 and 0.39 times the maximum applied stress.</p>			
Key words Crack growth, Crack closure, Finite elements, Elastic-plastic deformation, Cyclic loading, Fatigue, Three-dimensional analysis			
		Released for publication	
Distribution	FMV-FFL	Saab-Scania/L	KTH FFA
Copy No.	1-3	4-6	7 8-100